Journal of Cancer Research and Clinical Oncology (2019) 145:1179–1190
https://doi.org/10.1007/s00432-019-02865-8

ORIGINAL ARTICLE – CANCER RESEARCH

CD24 targeting bi-specific antibody that simultaneously stimulates NKG2D enhances the efficacy of cancer immunotherapy

Yue Han[1] · Fumou Sun[1] · Xinrong Zhang[1] · Tong Wang[1] · Jiahao Jiang[1] · Jialing Cai[1] · Qi Gao[1] · Kamal Hezam[1] · Yali Liu[1] · Jiajun Xie[1] · Min Wang[1] · Juan Zhang[1]

Received: 22 August 2018 / Accepted: 13 February 2019 / Published online: 18 February 2019

Abstract

Purpose Bi-specific antibody (BsAb) is an emerging novel format of antibody. We aimed to develop the natural killer (NK) cell receptor NK group 2, member D (NKG2D)-mediated, immune surveillance system. In this system, the NKG2D ligand MHC class I-related chain A (MICA) was fused with BsAb, which targeted a cluster of differentiation 24 (CD24), a tumor-initiating cell marker that is over-expressed on hepatocellular carcinoma (HCC).

Methods The Homo MICA extracellular domains (hMICA) were fused to the end of the heavy chain of cG7 with the flexible pentapeptide (Gly-Gly-Gly-Gly-Ser; G4S), which formed the cG7-MICA that was further identified using sodium dodecyl sulfate polyacrylamide gel electrophoresis (SDS–PAGE) and western blotting (WB). The targeting specificity was characterized using the Surface Plasmon Resonance (SPR) technology and a flow cytometry assay. Furthermore, the design of BsAb cG7-MICA that targeted CD24 and NKG2D was proven to enhance antibody-dependent, cell-mediated cytotoxicity (ADCC) in vitro by the CytoTox 96 Nonradioactive Cytotoxicity assay. Degranulation and a cytokine production assay of NK cells demonstrated that NK cells were activated effectively by cG7-MICA. Further, in HCC-bearing nude mice, the anti-tumor effects of cG7-MICA combined with sorafenib were verified again.

Results We purified cG7-MICA successfully, and it has a high affinity. In vivo, cG7-MICA recruited NK cells to the tumor site and improved the anti-tumor efficacy of sorafenib. cG7-MICA also activated NK cells to release interferon γ (IFN-γ) and tumor necrosis factor α (TNF-α), and it increased the CD107a expression on the surface of the NK cells in vitro.

Conclusion NK cells play a major role in the natural, innate immune system, and they have the function of identifying and killing target cells. cG7-MICA remodels the function of MICA molecules to activate NK cells, which provides a possible strategy for HCC-targeting immunotherapy.

Keywords BsAb · HCC · MICA · NK92 · NKG2D · Sorafenib

Introduction

Cancer immunotherapy is a new strategy for attacking cancer cells by stimulating the immune system of the patient. NK cells play an important role in the innate immune system and are the indispensable part of lymphocytes responsible for killing cancer cells (Li and Wang 2017). NKG2D is an activating receptor that is present on NK cells (Spear et al. 2013). When NKG2D binds with NKG2D ligands (NKG2DL) such as MICA or MICB on tumor cells (Waldhauer and Steinle 2008; Nausch and Cerwenka 2008), NK cells recognize tumor cells and release cytokines and some other tumor-killing particles to clear tumor cells (Zwirner et al. 2007). Nevertheless, tumor cells may avoid immune surveillance by shedding decoy NKG2D soluble ligands (Wu et al. 2004, 2009). To address this challenge, we designed a BsAb as an advanced solution for a dual targeting strategy within the same molecule that used NKG2DL to recruit NK-mediated immune surveillance.

✉ Min Wang
zhangjuan@cpu.edu.cn

✉ Juan Zhang
minwang@cpu.edu.cn

[1] Antibody Engineering Laboratory, State Key Laboratory of Natural Medicines, School of Life Science and Technology, China Pharmaceutical University, 154#, Tong Jia Xiang 24, Nanjing 210009, People's Republic of China

HCC is the most prevalent primary liver cancer and affects many people's physical health in the world (Qiu et al. 2017). High rates of CD24 expression have been found in primary HCC tissues (Huang et al. 1995). The expression of CD24 in primary HCC tissues is significantly higher than that in peritumor tissues and normal liver tissues (Yang et al. 2009). Studies have also shown that CD24 is critical for tumor differentiation, invasion, metastasis, and recurrence (Yang et al. 2009; Lee et al. 2011). Therefore, CD24 can be used as a marker to target liver cancer. Previously, we generated an antibody-ligand fusion rG7S-MICA that consisted of an anti-CD24 single-chain variable fragment (scFv) and MICA extracellular domains, and it effectively targeted the tumor site in HCC-bearing nude mice (Wang et al. 2016). However, the absence of the Fc segment in rG7s-MICA led to a short half-life, weak ADCC effects, and reduced anti-tumor efficacy (Ying et al. 2014). Hence, we designed a BsAb composed of antibody cG7 and MICA named cG7-MICA. When cG7-MICA bound to CD24 on HCC cells, these tumor cells were recognized by NK cells, and it triggered NK cell-mediated cytotoxicity (Claire et al. 2005; Xie et al. 2016). Meanwhile, the Fc segment bound to Fc receptors that were expressed on the surface of immune cells, such as NK cells and macrophages, which further triggered ADCC, complement-dependent cytotoxicity (CDC) effects, and an extended half-life after binding with neonatal receptors.

In this study, we aimed to generate a novel dual targeting antibody and to investigate further the anti-tumor activity against HCC, particularly the combo therapy of sorafenib, which is an antiangiogenic agent. The BsAb cG7-MICA could target HCC cells through the chimeric IgG1 antibody and activate NK cells to kill HCC cells by the associated MICA. Therefore, cG7-MICA might provide a new method and protocol for HCC therapy.

Materials and methods

Cell culture and animals

The human hepatoma cell lines Huh-7 and BEL-7402 preserved in our laboratory were cultured in high-glucose DMEM medium (Gibco, Grand Island, USA) that contained 10% (v/v) fetal bovine serum (FBS, Gibco, Grand Island, USA). The human NK cell line NK92 preserved in our lab was cultured in MEM-α medium (Gibco, Grand Island, USA) that contained 15% (v/v) FBS, 4.32% (*w*/*v*) Inositol, 0.78% (*w*/*v*) β-mercaptoethanol, 0.882% (*w*/*v*) folic acid, and 2×10^{-3}% (v/v) interleukin-2 (IL-2, Millipore, Temecula, USA). Cell culture media, trypsin powder, and supplements were purchased from Life Technologies (Basel, Switzerland). The BALB/C nude mice used in this study were purchased from Yangzhou University (Yangzhou, China). All animals were fed in a pathogen-free environment and were treated following the standards of the Comparative Medicine Centre of Yangzhou University.

Construction, expression, and purification of cG7 and cG7-MICA

The variable regions of heavy chain (H-chain) and light chain (L-chain) of cG7 were derived from the scFv rG7S. The human IgG1 full-length, constant region was from pUC57 preserved in our laboratory. The DNA sequence of Homo MICA extracellular domains (1–3) (hMICA) was synthesized after an optimization with CHO-biased codons (Genbank, NM_001289153.1). The amplified hMICA was linked to the 3′ end of the H-chain of cG7 with a G4S linker by overlap PCR, and the newly acquired fusion gene was named H′-chain. The light chain of cG7-MICA (L′-chain) retained the same gene as that of cG7 (L-chain). After digestion with NotI and EcoRI, the H′-chain and L′-chain were ligated with digested pMH3/pCApuro fragments separately, which formed pMH3-H′, pMH3-L′, pCApuro-H′, and pCApuro-L′.

The recombinant vectors (pMH3-H′, pMH3-L′, pCApuro-H′, and pCApuro-L′) were introduced into the CHO-s cell line with equal moles by electroporation. The high-yield stable clones were selected using 1 mg/mL G418 (Sigma–Aldrich) by Dot blot (HRP conjugated goat-anti-human IgG Fc, Sino Biological Inc., China). After fermentation of the high-yield stable clones, the culture supernatants were collected to purify fusion antibodies by a Protein A affinity chromatography column (GE Healthcare, Buckinghamshire, UK), followed by analysis using SDS–PAGE (10%) and Western blot assay.

Analysis of binding affinity using the Biacore system

The binding kinetics of cG7 and cG7-MICA to the CD24 mature peptide and cG7-MICA to NKG2D were measured with a Biacore system (Biacore X100, GE Healthcare, Sweden). Anti-Human IgG (Fc) antibody was immobilized on a sensor chip CM5 using a Human Antibody Capture Kit (GE Healthcare, Sweden). After cG7 and cG7-MICA were captured, soluble CD24 or NKG2D was injected at different concentrations into a running buffer (HBS-EP, pH 7.4). One flow cell of the sensor chip was set as a control. The captured antibody-analyte complex was removed by regeneration solution (3 mol/L of magnesium chloride). The association rate constant *ka* and dissociation rate constant *kd* were calculated and analyzed using the bivalent analyte model, and the equilibrium dissociation constant (*KD*) was calculated (*KD* = *kd*/*ka*).

Flow cytometry

To evaluate the targeting of the recombinant antibodies to hepatoma cells, BEL-7402 and Huh-7, 2×10^6 tumor cells were pre-incubated with 250 nM of samples and 5% skim milk as control at 4 °C for 1 h. This was followed by incubation with fluorescein isothiocyanate (FITC)-conjugated anti-human IgG (H + L) antibody (Miltenyi, Bergisch Gladbach, Germany) at 4 °C for 1 h. The cells were analyzed by flow cytometry (FACSCalibur, BD Biosciences, USA).

Antibody-dependent cellular cytotoxicity (ADCC)

The CytoTox 96 Nonradioactive Cytotoxicity assay (Promega, Madison, USA) was used for the cytotoxicity assay. Hepatoma cell lines Huh-7 or BEL-7402 were co-cultured with various amounts of peripheral blood mononuclear cells (PBMCs) or NK-92 cells in the presence of treatment of samples for 4 h at 37 °C. NK-92 cells or PBMCs were incubated with 1000 U/mL IL-2 for 24 h in advance. LDH analysis was performed according to the manufacturer's protocol. Controls for spontaneous LDH release in effector or target cells, as well as target maximum release, were prepared. The percentage of cell lysis was calculated as: % Cytotoxicity = [(experimental − effector spontaneous − target spontaneous)/(target maximum − target spontaneous)] × 100.

Degranulation and cytokine production assay of NK cells

NK92-FcR cells were pretreated with recombinant human interleukin-2 (IL-2, Millipore, Temecula, USA) for 24 h; then, these cells were co-incubated with hepatoma cell lines Huh-7 or BEL-7402 for 4 h at an effector-target (E:T) ratio of 10:1 in the presence of various concentrations of samples. The degranulated NK92-FcR cells were detected using flow cytometry based on the release of LAMP-1 (CD107a). Meanwhile, the supernatant of co-incubated cells was collected for the quantification of IFN-γ and TNF-α using an enzyme-linked, immunosorbent assay (ELISA) kit (KeyGEN, Nanjing, China).

Anti-tumor efficacy in xenograft tumor models

An aliquot of 1×10^7 HCC cells was injected subcutaneously into the left armpit of each 5-week-old BALB/c nude mice. After average tumor volume reached 100 mm^3, the tumor-bearing mice were divided randomly into six groups, with six mice in each group, and administered every other day. The anti-tumor efficacy of cG7-MICA was evaluated compared with that of 5.0 mg/kg cG7 (high dose), 5.0 mg/kg rG7s-MICA (high dose), and 20 mg/kg sorafenib (intragastric administration). PBS was set as the control group. A combination of cG7-MICA (5.0 mg/kg) with sorafenib (20 mg/kg) was investigated to determine whether that produced a better anti-tumor effect. Tumor development in nude mice was measured every other day and the tumor volume was calculated with the formula: $V = LW^2/2$ (L longest diameter of tumor, W maximum transverse diameter of vertical direction). The mice were killed 3 weeks after treatment, and tumor tissues were prepared for further analysis. A survival model was set using the same cell line, in which four groups of mice were equally treated with PBS, cG7, cG7-MICA, and the combination of cG7-MICA and sorafenib, separately. The mice were killed when tumors reached 2000 mm^3 as per institutional guidelines to determine the survival.

Immunohistochemistry and immunofluorescence analysis

Paraffin sections were cut into 5 μm sections and fixed in 4% paraformaldehyde. For immunohistochemical (IHC) staining, the sections were incubated with the CD49b antibody (Abcam, Cambridge, UK) and the Ki-67 antibody (Cell Signaling Technology, Boston, USA) separately. The sections were incubated with horseradish, peroxidase-labeled, secondary antibody and analyzed with a Vectastain ABC Kit (Dako, Copenhagen, Denmark). For immunofluorescence (IF) staining, the sections were incubated with IFN-γ or TNF-α antibody (Abcam, Cambridge, UK) and Alexafluor-488/594 labeled antibody (Molecular Probes, Eugene, USA). The slides were mounted with Vectashield mounting media that contained DAPI and analyzed under a fluorescence microscope.

Statistical analysis

Statistical analysis was performed using SPSS 20.0 and GraphPad Prism software. All data were presented as the mean ± SD from at least three independent experiments. Differences between multiple groups were analyzed by Tukey's multiple comparison test. A p value < 0.05 was considered as a significant difference.

Results

Construction and identification of cG7 and cG7-MICA

The construction and illustration of full-length antibody cG7 and fusion BsAb cG7-MICA were denoted with a flow diagram (Fig. 1a, b). The recombinant expression vectors of cG7 or cG7-MICA were co-transfected into CHO-s cells by electroporation. Then, three stably transfected clones with high expression levels were obtained through two rounds

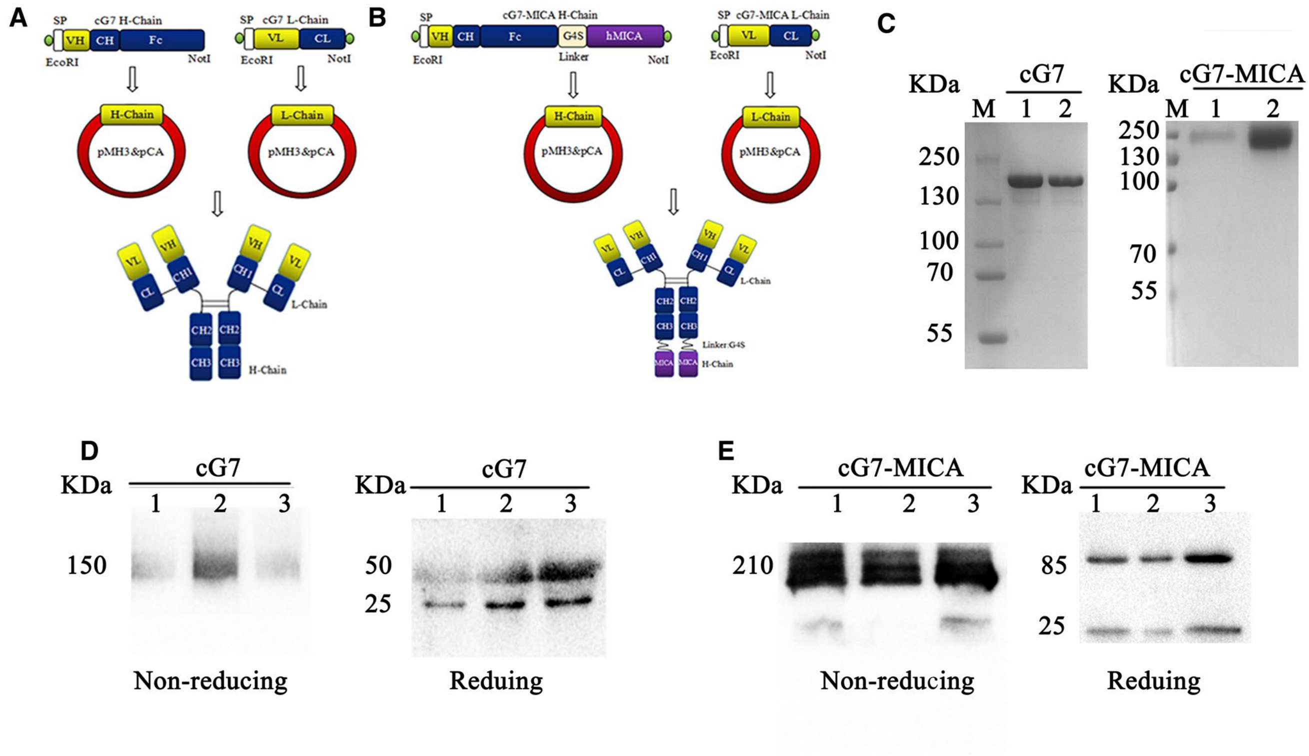

Fig. 1 Construction and identification of cG7 and cG7-MICA. **a, b** Diagram of the construction and structure of cG7 and cG7-MICA. **c** SDS–PAGE analysis for the molecular weight of purified cG7 and cG7-MICA. *M* Protein markers. Lane 1, 2: samples. **d, e** Non-reducing and reducing Western blot analysis for the assembly of purified cG7 and cG7-MICA. *M* Protein markers; Lane 1, 2, 3: samples that were amplified and purified from three stably transfected clones with high expression levels

of screenings with 1 mg/mL G418. The expressed recombinant antibodies cG7 and cG7-MICA were purified with a Protein A affinity chromatography column. SDS–PAGE analysis indicated the expected molecular weight of 150 kD for cG7 and 210 kD for cG7-MICA (Fig. 1c). The Western blot results demonstrated that the target antibodies were assembled correctly in CHO-s cells (Fig. 1d, e).

Determination of binding affinity of full-length antibody cG7 and bi-specific antibody cG7-MICA

The antibody was identified for its ability to target and to bind. The equilibrium dissociation constant (KD) value between cG7/cG7-MICA and the CD24 mature peptide was measured with the Biacore system using the 2:1 binding model. Full-length antibody cG7 exhibited high affinity to the CD24 mature peptide [ka (1/Ms): 1.76E+06; kd (1/s): 3.36E-04; KD (M): 1.91E-10] (Fig. 2a), which was much higher than scFv rG7s that was constructed earlier (Wang et al. 2016). cG7-MICA [ka (1/Ms): 1.40E+06; kd (1/s): 3.39E-04; KD (M): 2.42E-10] showed non-decreased specificity and affinity to CD24 compared with cG7 (Fig. 2b). The KD value between cG7-MICA and soluble NKG2D [ka (1/Ms): 2.62E+03; kd (1/s): 1.5E-03; KD (M): 5.76E-07] was also evaluated (Fig. 2c). cG7-MICA was able to target CD24 and NKG2D, which displayed the binding capacity of cG7-MICA at the molecular level.

Hepatoma carcinoma cells Huh-7 and BEL-7402 were typical CD24 over-expressing tumor cells. Huh-7 and BEL-7402 cells expressed low levels of membrane MICA and no membrane NKG2D on these cell lines. High expression levels of CD24 were detected in >90% of Huh7 and BEL-7402 cells, which had been demonstrated previously (Wang et al. 2016). After the shRNA silenced the CD24 molecules on the surface of the tumor cells, the binding affinity between the scFv rG7s and the tumor cells was obviously reduced (Wang et al. 2016), which indicated that the antibody was bound to CD24 on the surface of the tumor cells specifically. Furthermore, the binding of cG7 and cG7-MICA to the tumor cell lines Huh-7 and BEL-7402 was determined using flow cytometry. cG7 and cG7-MICA had revealed the similar binding ability to these two human hepatoma cell lines, which was much higher than that of scFv rG7s. These results revealed that cG7-MICA had much higher binding affinity than scFv rG7s and non-decreasing binding affinity to CD24 molecules when the extracellular region of hMICA was linked to the Fc fragment of cG7 (Fig. 2d).

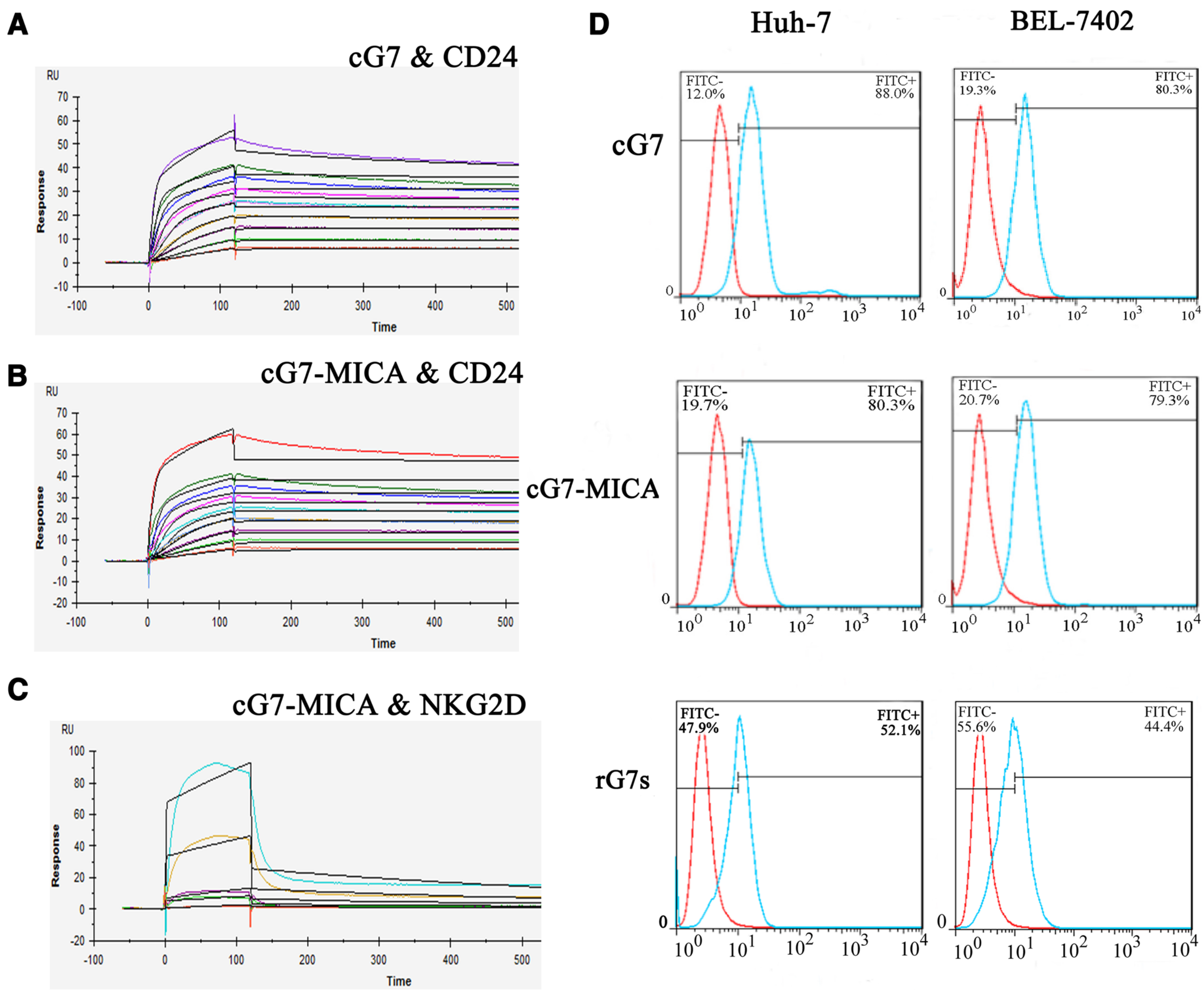

Fig. 2 Binding affinity of cG7 and cG7-MICA. **a** Set of sensorgrams of CD24 binding with cG7. The association rate increased with increasing concentration of CD24 (from bottom to top), which ranged from 0.390625 to 100 nmol/L. The complex dissociated when buffer flowed through at 120 s. KD (M): 1.91E-10. **b** Set of sensorgrams of CD24 binding with cG7-MICA. The concentration of CD24 (from bottom to top) ranged from 0.390625 to 100 nmol/L. KD (M): 2.42E-10. **c** Set of sensorgrams of NKG2D binding with cG7-MICA. The concentration of NKG2D (from bottom to top) ranged from 6.25 to 100 nmol/L. KD (M): 5.76E-07. **d** cG7-MICA and cG7 showed similar affinity to CD24 over-expressing Huh-7 and BEL-7402. The binding rate was 80.3% between cG7-MICA and Huh-7 and 79.3% between cG7-MICA and BEL-7402, which was higher than that of rG7s

cG7-MICA enhanced PBMCs or NK cell cytotoxicity through the MICA-NKG2D/Fc-FcR pathway

The cytotoxicity assay was performed using Huh-7 or BEL-7402 cells as the target cells and NK92-FcR cells or PBMCs as the effector cells. NK92 cells or PBMCs were incubated with 1000 U/mL IL-2 for 24 h, and then they were co-cultured with BEL-7402 or Huh-7 cells in the presence of an optimal concentration of cG7-MICA (10 μg/mL) for 4 h at 37 °C. cG7-MICA triggered strong cytotoxicity on Huh-7 and BEL-7402 cells in an E:T ratio-dependent manner. However, cG7 displayed a relatively lower ability for tumor cell lysis due to the absence of the MICA fragment. Simultaneously, cG7-MICA induced higher cell lysis compared with rG7S-MICA because of the fusion with the Fc region. The specific lysis of Huh-7 or BEL-7402 was reduced after adding free soluble hMICA to the supernatant, which indicated that free soluble hMICA weakened the cytotoxicity of PBMCs or NK92-FcR cells (Fig. 3a–d). Previous research results found that the binding of rG7S-MICA to NK92-FcR cells was significantly decreased after NKG2D knockdown from the NK92-FcR cells, and the silencing of NKG2D caused reduced tumor-killing efficacy of NK92-FcR cells that were mediated by rG7S-MICA in high E:T

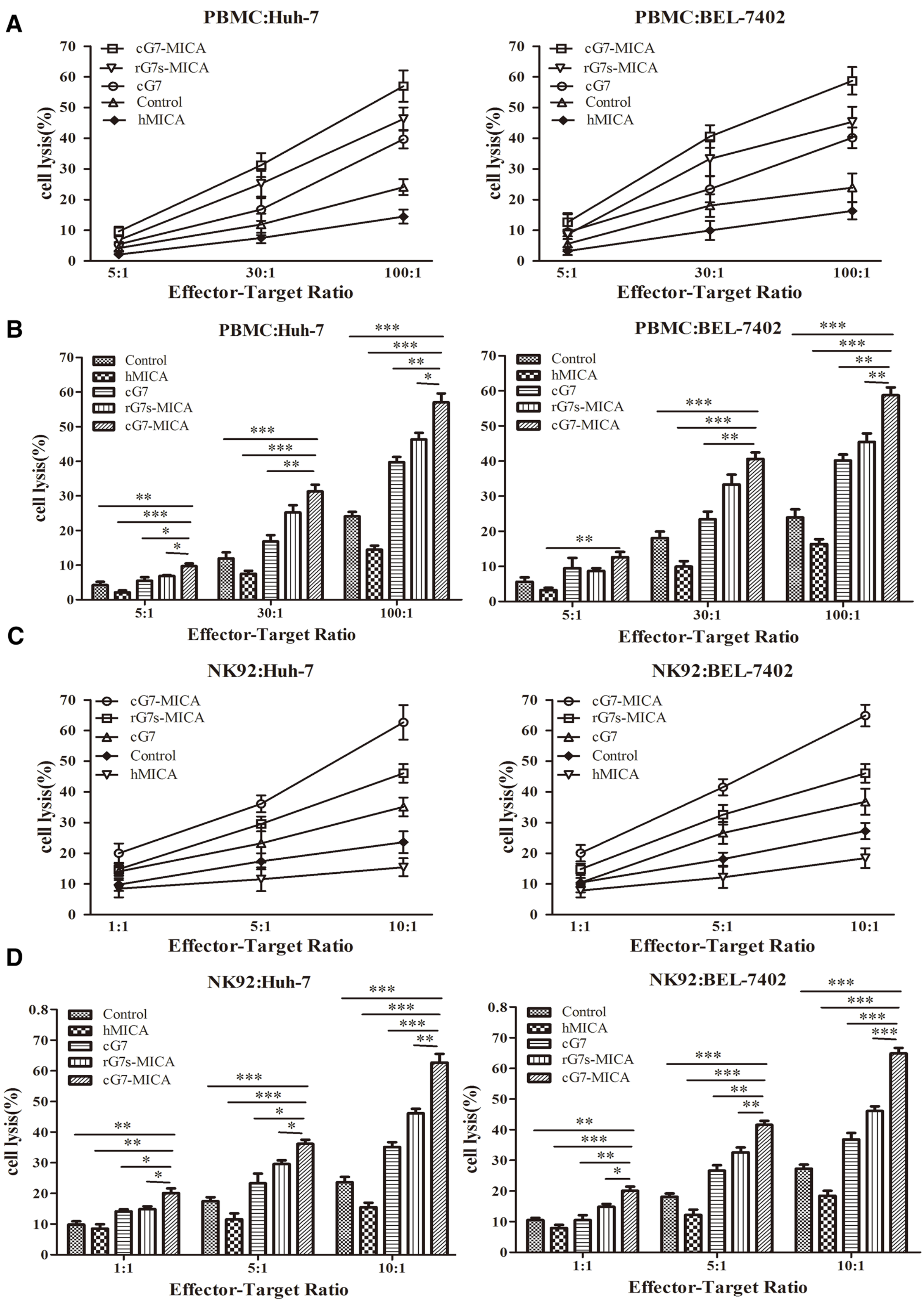
A
PBMC:Huh-7
PBMC:BEL-7402
cG7-MICA
rG7s-MICA
cG7
Control
hMICA
cell lysis(%)
Effector-Target Ratio
5:1
30:1
100:1
B
PBMC:Huh-7
PBMC:BEL-7402
C
NK92:Huh-7
NK92:BEL-7402
1:1
5:1
10:1
D
NK92:Huh-7
NK92:BEL-7402

◀**Fig. 3** cG7-MICA enhanced PBMCs or cytotoxicity of NK92-FcR cells through the MICA/NKG2D and Fc/FcR pathways. **a**, **c** PBMCs and NK92-FcR cells stimulated by 1000 U/mL IL-2 were incubated with Huh-7 or BEL-7402 at E:T ratios of 5:1, 30:1, and 100:1 in the presence of an optimal concentration of cG7-MICA for 4 h. The equivalent dose of cG7 and rG7S-MICA were used as a comparative group. At the same time, the equivalent dose of recombinant MICA (rMICA) was used as the blocking group. **b**, **d** *T* test analysis indicated significant enhancement of target cell lysis induced by cG7-MICA at high E:T ratio of 100:1 for PBMCs and NK92 cells. Data were given as the mean ± SD ($n = 3$). $^{*}p < 0.05$, $^{**}p < 0.01$, $^{***}p < 0.001$, compared with the cG7-MICA group

ratios (Wang et al. 2016). We concluded, therefore, that cG7-MICA effectively activated PBMCs or NK cells through the MICA/NKG2D and Fc/FcR pathways and enhanced PBMCs and NK cell-mediated cytotoxicity.

cG7-MICA promoted NK cells to degranulate and to release IFN-γ and TNF-α

To verify how cG7-MICA treatment triggered the NKG2D and FcR-mediated killing effects on tumor cells, the degranulation of NK92-FcR cells was detected using LAMP-1 (CD107a) as a marker. NK92-FcR cells were incubated with 1000 U/mL IL-2 for 24 h, and then co-cultured with Huh-7 cells at an effector-target (E:T) ratio of 10:1, which followed the treatment with different samples at the same concentration of 10 μg/mL. FACS analysis revealed that cG7-MICA more easily stimulated the expression of CD107a on NK92-FcR cells than cG7 and rG7s-MICA after activating the NK92-FcR cells through the NKG2D and FcR pathways (Fig. 4a, b).

Meanwhile, the supernatant of NK92-FcR cells, which were co-incubated with BEL-7402 or Huh-7 cells, was collected for the quantification of IFN-γ and TNF-α using an ELISA kit after being treated with 10 μg/mL of cG7-MICA. In correspondence with the results of the FACS analysis, the ELISA assay showed that cG7-MICA promoted a greater release of IFN-γ and TNF-α by NK92-FcR than other samples (Fig. 4c, d). We concluded that NK92-FcR cells were effectively activated by cG7-MICA to up-regulate CD107a expression, which occurred in proportion to the secretion of perforin, and they released cytokines such as IFN-γ and TNF-α to exert anti-tumor activity.

cG7-MICA enhanced the anti-tumor efficacy of sorafenib in vivo

BALB/c nude mice with subcutaneously transplanted Huh-7 cells were divided randomly into groups of six mice and treated with different samples (PBS, cG7, rG7s-MICA, cG7-MICA, sorafenib, and combination of cG7-MICA and sorafenib).Tumor volume (Fig. 5a) and tumor weight (Fig. 5b, c) in Huh-7-bearing nude mice were measured to evaluate the anti-tumor activity of cG7-MICA co-administered with sorafenib in vivo. On the observation of survival, cG7-MICA treatment significantly extended the survival of Huh-7 xenografted nude mice compared with cG7-treated group. In addition, the combination of cG7-MICA and sorafenib had better efficacy than other treatments (Fig. 5d). In addition, we evaluated proliferation of tumor cells based on the expression level of Ki-67 in the tumor tissue by an immunohistochemistry experiment (Fig. 5e, f). As expected, the group treated with cG7-MICA combined with sorafenib had the most obvious anti-tumor effects. The results also suggested that the group treated with cG7-MICA showed superior anti-tumor efficacy compared with that of cG7 or rG7s-MICA, which was consistent with the results in vitro.

cG7-MICA recruited NK cells and enhanced the release of cytokines

To further demonstrate that cG7-MICA recruited NK cells, immunohistochemistry and immunofluorescence were used to monitor NK infiltration and cytokine release by NK cells in Huh-7 solid tumor tissue. After treatment with cG7-MICA, the proportion of $CD49b^{+}$ NK cells in tumor tissue was significantly increased compared with the control (Fig. 6a, b). Furthermore, we found that cG7-MICA significantly increased the secretion of IFN-γ and TNF-α by NK cells compared with cG7 or rG7s-MICA (Fig. 6c, d). These results again illustrated why cG7-MICA had superior anti-tumor efficacy in vivo. In conclusion, cG7-MICA strengthened NK cell-mediated immunosurveillance and Fc-mediated ADCC and CDC effects, and cG7-MICA showed improved bio-activity compared with cG7 or rG7s-MICA.

Discussion

We had previously designed a BsAb rG7s-MICA by fusing the extracellular domains of hMICA with the C-terminus of scFv rG7s through a G4S linker. rG7s was derived from a murine monoclonal antibody developed by our group, and it specifically recognized the tumor-associated CD24. However, single-chain antibodies have low affinity to their antigens, and they lack ADCC and CDC effects. We, therefore, generated the second generation of anti-CD24, bi-specific antibody cG7-MICA. cG7 is a chimeric anti-CD24 antibody. The newly constructed bi-specific antibody cG7-MICA enhanced ADCC effects mainly by activating NK cells, which played a fundamental role in innate immunity. When cG7-MICA recognized and bound to CD24, the recombinant MICA molecules were displayed indirectly on the surface of Huh-7 and BEL-7402 hepatocarcinoma cells, which compensated for the shedding MICA.

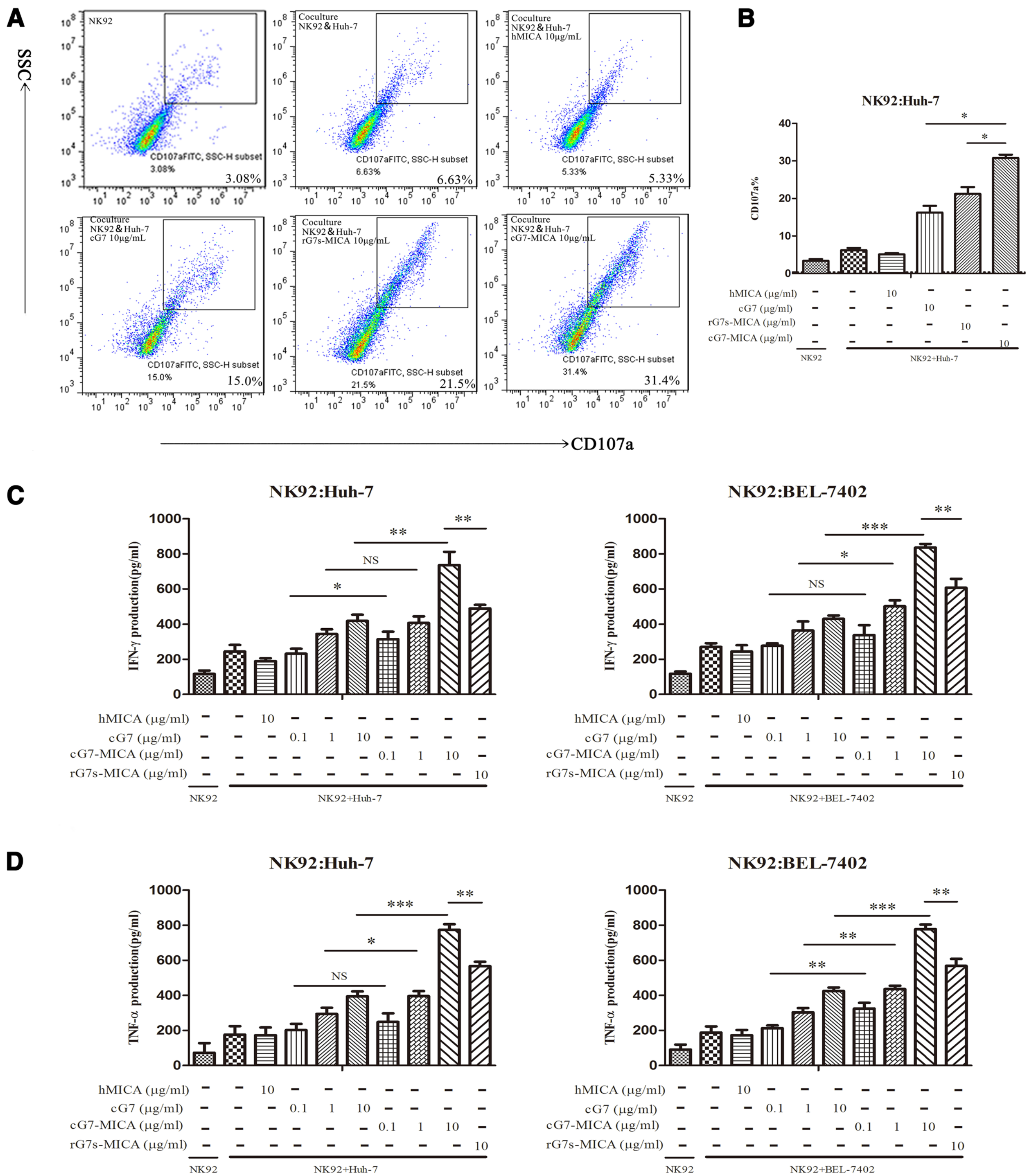

Fig. 4 cG7-MICA promoted NK92-FcR cells to degranulate and to release IFN-γ and TNF-α. **a** Flow cytometry analysis of the degranulation of NK92-FcR cells stimulated by IL-2 based on the expression level of CD107a after exposure to Huh-7 cells at an E:T ratio of 10:1 in the presence of an optimal concentration of different samples for 4 h. **b** *T* test revealed that cG7-MICA stimulated the expression of CD107a better compared with cG7 and rG7s-MICA after activating the NK92-FcR cells. **c, d** The release of IFN-γ and TNF-α by NK92-FcR cells after exposure to Huh-7or BEL-7402 cells at an E:T ratio of 10:1 in the presence of different samples for 4 h was assessed by an ELISA kit. cG7 and cG7-MICA promoted the release of IFN-γ and TNF-α by NK92-FcR in a dose-dependent manner, and cG7-MICA displayed obvious improvement on the releasing level of IFN-γ and TNF-α compared with cG7 and rG7s-MICA. Data were given as the mean ± SD ($n=3$). $*p<0.05$, $**p<0.01$, $***p<0.001$, *NS* no significance

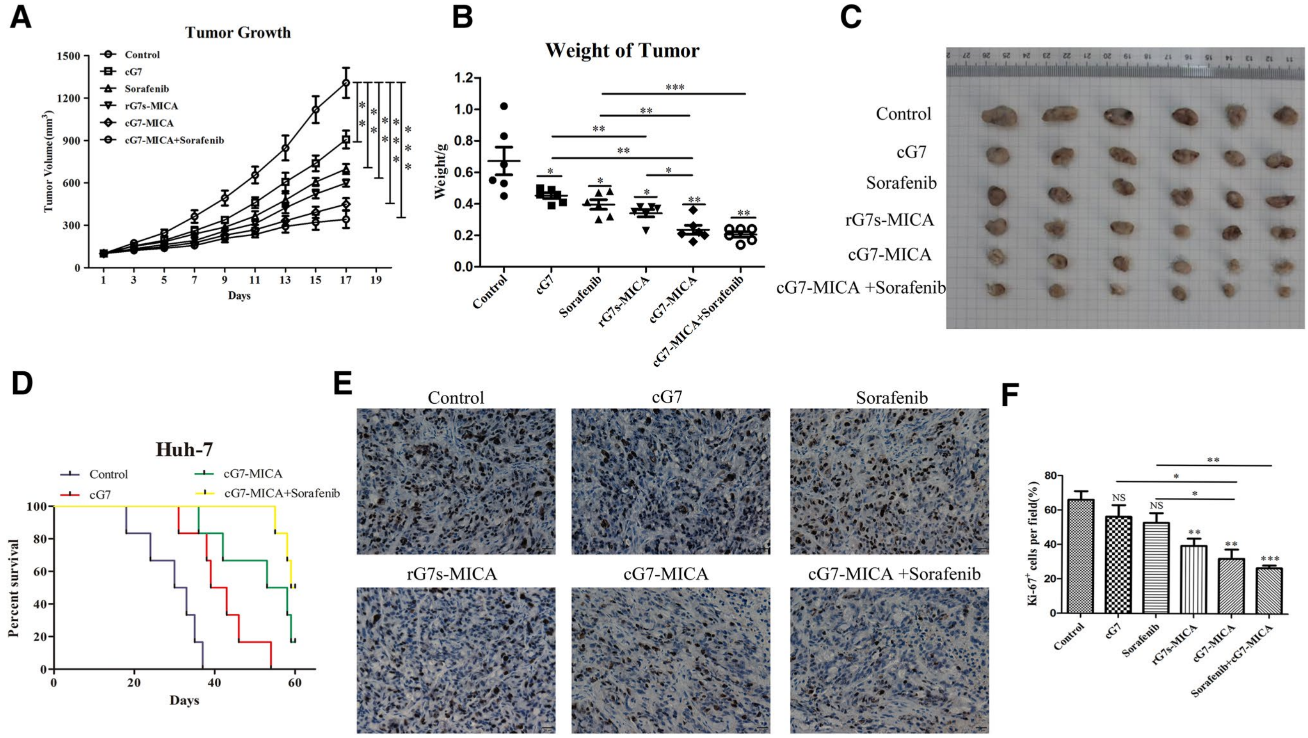

Fig. 5 cG7-MICA enhanced the anti-tumor efficacy of sorafenib in vivo. **a** Tumor growth curve of different groups that were treated with PBS, cG7, sorafenib, rG7s-MICA, cG7-MICA, and cG7-MICA combined with sorafenib. **b** The average tumor weight of each group was different. cG7-MICA inhibited tumor growth more obviously than cG7 and rG7s-MICA. In addition, it improved the anti-tumor effect of sorafenib to a great extent. **c** The image of the tumor mass showed the results visually. **d** The survival of Huh-7-bearing mice after a 60-day tumor challenge in each group. cG7-MICA treatment significantly extended the survival of Huh-7-bearing nude mice compared with cG7 treated group. In addition, the combination of cG7-MICA and sorafenib had better efficacy than other treatments. **e, f** The immunohistochemical (IHC) staining of Ki-67 (brown staining) from tumor tissue was reduced from about 70–25% after treatment with sorafenib combined with cG7-MICA. Ki-67 expression reflected the proliferation of tumor cells. Data were given as the mean ± SD ($n = 6$ in tumor growth and the survival model experiment, $n = 5$ in IHC). $^{*}p < 0.05$, $^{**}p < 0.01$, $^{***}p < 0.001$, *NS* no significance

Hepatocellular carcinoma (HCC) ranks as the fifth most common cancer and the second leading cause of cancer deaths worldwide (Fathy et al. 2017). Most of the current therapeutic antibodies, which include bevacizumab (Avastin) and cetuximab, show limited efficacy against HCC as a single agent. Sorafenib, which is the only molecular targeting agent approved by the FDA for liver cancer, is a multi-kinase inhibitor. Preclinical studies have shown that sorafenib can simultaneously inhibit a variety of kinases expressed intracellularly or on the surface of cell membranes, which include RAF kinase, vascular endothelial growth factor receptor-2 (VEGFR-2), vascular endothelial growth factor receptor-3 (VEGFR-3), platelet-derived growth factor receptor-β (PDGFR-β), and others (Lin et al. 2017; Turcios et al. 2017). It is currently used at a dose of 400 mg twice daily in clinical treatment. Given the fact that a high dose leads to serious side effects, it is still facing the problems of poor anti-tumor effects and drug resistance (Shruthi et al. 2018). Sorafenib resulted in the up-regulation of pSTAT 3 (Tai et al. 2011). Interestingly, CD24 increased the expression of STAT3-dependent target genes (Chen et al. 2017). Hence, we hypothesized that the combination of cG7-MICA and sorafenib could improve the anti-tumor efficacy of sorafenib.

To investigate the immunomodulatory properties of cG7-MICA, both the NK cell line (NK92-FcR cells) and human PBMCs were studied as effector cells, and tumor cells (Huh-7, BEL-7402) were studied as target cells (Arai et al. 2008). The results showed that cG7-MICA had a superior ADCC effect compared with cG7, and the fused MICA molecules promoted the degranulation of NK cells, which were further proved by a flow cytometry assay. In addition, increased IFN-γ and TNF-α were detected. In comparison with rG7s-MICA, cG7-MICA possessed higher anti-tumor activity, which indicated that a Fc module was necessary for CD24-based, monoclonal antibody therapy. In contrast, soluble recombinant hMICA exerted weaker cytotoxicity than the control group, which suggested that the binding of soluble MICA to membrane NKG2D blocked the recognition of NK cells with tumor cells and, hence, attenuated the activation of NK cells. For one reason, a physical stereo-hindrance effect on NK cells hindered the capture of tumor cells. For the other, soluble MICA interacted with NKG2D on NK

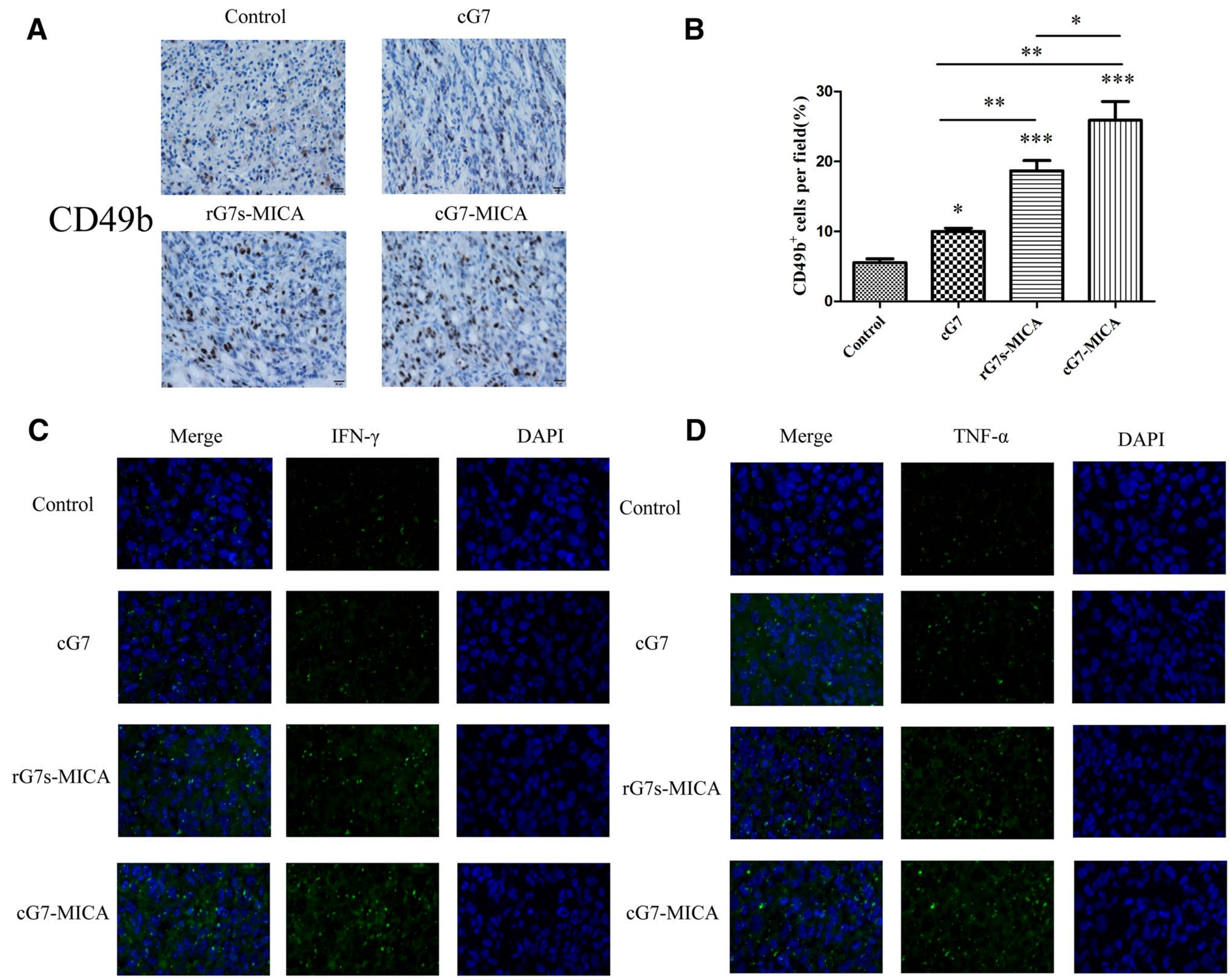

Fig. 6 cG7-MICA recruited NK cells and enhanced the release of cytokines into the tumor. **a, b** CD49b is a biomarker on NK cells from mice, and the immunohistochemical (IHC) staining of CD49b$^+$ cells demonstrated that cG7-MICA recruited NK cells to tumor tissue. **c, d** Immunofluorescence staining of the levels of IFN-γ and TNF-α (green fluorescence) released by CD49b$^+$ NK cells in different groups. The increased secretion of IFN-γ and TNF-α indicated that more NK cells were gathering in the tumor tissue and were activated. Data were given as the mean ± SD ($n = 5$). $^*p < 0.05$, $^{**}p < 0.01$, $^{***}p < 0.001$, *NS* no significance

cells, which inhibited the MICA/NKG2D-mediated cytotoxicity. This result was consistent with the fact that tumor cells can escape the immune surveillance of activated NK cells when there was an increase in soluble MICA in patient blood (Wu et al. 2004, 2009).

To further validate the in vivo anti-tumor activity of cG7-MICA, we established xenograft tumor models. BALB/c nude mice lacked thymic function and T cells, but maintained NK cell activity (Ambade and Mulherkar 2008; Budzynsk and Radzikowski 1994). The MICA segment of the fusion antibody cG7-MICA not only recognizes human NKG2D receptors, but it also recognizes murine NKG2D receptors (Rothe et al. 2014), which allows for the possibility for xenograft tumor models in vivo. After the administration, the tumor growth was effectively restrained. The combination of cG7-MICA and sorafenib contributed to the highest anti-tumor efficacy and longer survival of tumor-bearing nude mice, which is in line with what we expected. NK cells at the tumor site were efficiently recruited either through the interaction between NKG2D and MICA or between Fc and FcR, which resulted in an increased release of IFN-γ and TNF-α.

The results of the experiments above revealed that the binding of MICA molecules to antibodies effectively remodeled the function of MICA, which is a possible strategy for solving the problems caused by the shedding of MICA from the tumor cells. To address this challenge in another way, Lucas Ferrari de Andrade designed an antibody that targeted and inhibited the proteolytic shedding of MICA such that the antibody treatment not only locked MICA and MICB proteins onto the cancer cells, but also promoted NK cell infiltration for elimination of cancer cells (Lucas et al. 2018). Regardless of the method we used, the purpose was to activate NK cells through the MICA/NKG2D pathway. NK cells play an important role in immune surveillance (Malmberg et al. 2017; Tian 2017). It is increasingly recognized that the NK cell line is a heterogeneous population of innate lymphoid cells (ILC) (Peng and Sun 2017). Increasing evidence shows that NK cells have immune memory (Geary and Sun 2017). After NK cells are activated, they differentiate partially into memory cells. Target cells can, therefore, be identified and killed more quickly and effectively. Hence, we chose NK cells as the focus of our study. In conclusion, we expect that the design of fusing MICA molecules with any antibody can provide an effective therapeutic strategy against malignants.

Acknowledgements Thank Thomas A. Gavin, Professor Emeritus, Cornell University, for help with editing this paper.

Funding This study was supported by the National Natural Science Foundation of China (NSFC81473125) and the Natural Science Foundation of Jiangsu Province (BK20161459), Jiangsu Province Qinglan Project (2014).

Compliance with ethical standards

Conflict of interest The authors declare no competing financial interests.

Ethical approval All experimental procedures were conducted in conformity with institutional guidelines for the care and use of laboratory animals in Yangzhou University, Yangzhou, China, and they conformed to the National Institutes of Regulations for the Administration of Affairs Concerning Experimental Animals.

References

Ambade A, Mulherkar R (2008) Adoptive T cell transfer augments IL-2 mediated tumor regression in a HNSCC xenograft nude mouse model. Cancer Lett 272(2):316–324. https://doi.org/10.1016/j.canlet.2008.07.023

Arai S, Meagher R, Swearingen M, Myint H, Rich E, Martinson J, Klingemann H (2008) Infusion of the allogeneic cell line NK-92 in patients with advanced renal cell cancer or or melanoma: a phase I trial. Cytotherapy 10(6): 625–632. https://doi.org/10.1080/14653240802301872

Budzynski W, Radzikowski C (1994) Cytotoxic cells in immunodeficient athymic mice. Immunopharmacol Immunotoxicol 16:319–346. https://doi.org/10.3109/08923979409007097

Chen ZG, Wang T, Tu XJ, Xie W, He H, Wang M, Zhang J (2017) Antibody-based targeting of CD24 enhances antitumor effect of cetuximab via attenuating phosphorylation of Src/STAT3. Biomed Pharmacother 90:427–436. https://doi.org/10.1016/j.biopha.2017.03.094

Claire G, Larbouret C, Cesson V, Donda A, Held W, Mach J-P, Pelegrin A Robert B, (2005) MHC Class I-related chain A conjugated to antitumor antibodies can sensitize tumor cells to specific lysis by natural killer cells. Clin Cancer Res 11(20):7516–7522. https://doi.org/10.1158/1078-0432.CCR-05-0872

Fathy AH, Bashandy AM, Bashandy SA, Mansour AM, Elsadek B (2017) Sequential analysis and staging of a diethylnitrosamine induced hepatocellular carcinoma in male Wistar albino rat model. Can J Physiol Pharmacol 95:1462–1472. https://doi.org/10.1139/cjpp-2017-0413

Geary CD, Sun JC (2017) Memory responses of natural killer cells. Semin Immunol 31:11–19. https://doi.org/10.1016/j.smim.2017.08.012

Huang LR, Hsu HC (1995) Cloning and expression of CD24 gene in human hepatocellular carcinoma A potential early tumor marker gene correlates with p53 mutation and tumor differentiation. Can Res 55:4717–4721

Lee TK, Castilho A, Cheung VC, Tang KH, Ma S, Ng IO (2011) CD24(+) liver tumor-initiating cells drive self-renewal and tumor initiation through STAT3-mediated NANOG regulation. Cell Stem Cell 9(1):50–63. https://doi.org/10.1016/j.stem.2011.06.005

Li D, Wang W (2017) Booming cancer immunotherapy fighting tumors. Sci China Life Sci 12:1445–1449. https://doi.org/10.1007/s11427-017-9208-1

Lin S, Hoffmann K, Gao C, Petrulionis M, Herr I, Schemmer P (2017) Melatonin promotes sorafenib induced apoptosis through synergistic activation of JNK/c-jun pathway in human hepatocellular carcinoma. J Pineal Res 62(3):12398–12420. https://doi.org/10.1111/jpi.12398

Lucas AF de, Tay RE, Pan D, Adrienne M, Luoma, Kai W, Wucherpfennig. (2018)Antibody-mediated inhibition of MICA and MICB shedding promotes NK cell–driven tumor immunity. Science 359:1537–1542. https://doi.org/10.1126/science.aao0505

Malmberg KJ, Carlsten M, Björklund A, Sohlberg E, Bryceson YT, Ljunggren HG (2017) Natural killer cell-mediated immunosurveillance of human cancer. Semin Immunol 31:20–29. https://doi.org/10.1016/j.smim.2017.08.002

Nausch N, Cerwenka A (2008) NKG2D ligands in tumor immunity. Oncogene 27(45):5944–5958. https://doi.org/10.1038/onc.2008.272

Peng H, Sun R (2017) Liver-resident NK cells and their potential functions. Cell Mol Immunol 14:890–894.w33. https://doi.org/10.1038/cmi.2017.72

Qiu L, Tang Q, Li G, Chen K (2017) Long non-coding RNAs as biomarkers and therapeutic targets: recent insights into hepatocellular carcinoma. Life Sci 191:273–282. https://doi.org/10.1016/j.lfs.2017.10.007

Rothe A, Jachimowicz RD, Borchmann S, Madlener M, Keßler J, Reiners KS, Sauer M, Hansen HP, Ullrich RT, Chatterjee S, Borchmann P, Yazaki P, Koslowsky TC, Engert A, Heukamp LC, Hallek M, Strandmann EP von (2014) The bispecific immunoligand ULBP2-aCEA redirects natural killer cells to tumor cells and reveals potent anti-tumor activity against colon carcinoma. Int J Cancer 134(12):2829–2840. https://doi.org/10.1002/ijc.28609

Shruthi K, Makol A, Anuradha C (2018) Sorafenib response in hepatocellular carcinoma: microRNAs as tuning forks. Hepatol Res 48:5–14. https://doi.org/10.1111/hepr.12991

Spear P, Wu MR, Sentman ML, Sentman CL (2013) NKG2D ligands as therapeutic targets. Cancer Immun 13(2):8–21

Tai WT, Cheng AL, Shiau CW, Huang HP, Huang JW, Chen PJ, Chen KF (2011) Signal transducer and activator of transcription 3 is a major kinase-independent target of sorafenib in hepatocellular carcinoma. J Hepatol 55(5):1041–1048. https://doi.org/10.1016/j.jhep.2011.01.047

Tian Z (2017) NK cells and Immunotherapy. Semin Immunol 31:1–2. https://doi.org/10.1016/j.smim.2017.09.008

Turcios L, Vilchez V, Acosta LF, Poyil P, Butterfield DA, Mitov M, Marti F, Gedaly R (2017) Sorafenib and FH535 in combination act synergistically on hepatocellular carcinoma by targeting cell bioenergetics and mitochondrial function. Dig Liver Dis 49:697–704. https://doi.org/10.1016/j.dld.2017.01.146

Waldhauer I, Steinle A (2008) NK cells and cancer immunosurveillance. Oncogene 27(45):5932–5943. https://doi.org/10.1038/onc.2008.267

Wang T, Sun F, Xie W, Tang M, He H, Jia X, Tian X, Wang M, Zhang J (2016) A bispecific protein rG7S-MICA recruits natural killer cells and enhances NKG2D-mediated immunosurveillance against hepatocellular carcinoma. Cancer Lett 372(2):166–178. https://doi.org/10.1016/j.canlet.2016.01.001

Wu JD, Higgins LM, Steinle A, Cosman D, Haugk K, Plymate SR (2004) Prevalent expression of the immunostimulatory MHC class I chain–related molecule is counteracted by shedding in prostate cancer. J Clin Investig 114(4):560–568. https://doi.org/10.1172/JCI200422206

Wu JD, Atteridge CL, Wang X, Seya T, Plymate SR (2009) Obstructing shedding of the immune stimulatory micb prevents tumor formation: implication for targeted cancer therapy. Clin Cancer Res 15(2):632–640. https://doi.org/10.1158/1078-0432.CCR-08-1305

Xie W, Liu F, Wang Y, Ren X, Wang T, Chen Z, Tang M, Sun F, Li Z, Wang M, Zhang J (2016) VEGFR2 targeted antibody fused with MICA stimulates NKG2D mediated immunosurveillance and exhibits potent anti-tumor activity against breast cancer. Oncotarget 7(13):16445–16461

Yang XR, Xu Y, Fan J et al (2009) CD24 is a novel predictor for poor prognosis of hepatocellular carcinoma after surgery. Clin Cancer Res 15(17):5518–5527. https://doi.org/10.1158/1078-0432.CCR-09-0151

Ying T, Gong R, Ju TW, Prabakaran P, Dimitrov DS (2014) Engineered Fc based antibody domains and fragments as novel scaffolds. Biochim Et Biophys Acta 1844(11):1977–1982. https://doi.org/10.1016/j.bbapap.2014.04.018

Zwirner NW, Fuertes MB, Girart MV, Domaica CI, Rossi LE (2007) Cytokine-driven regulation of NK cell functions in tumor immunity: role of the MICA-NKG2D system. Cytokine Growth Factor Rev 18(1):159–170. https://doi.org/10.1016/j.cytogfr.2007.01.013